Multi-time-scale hydroclimate dynamics of a regional watershed and links to large-scale atmospheric circulation: Application to the Seine river catchment, France

Massei, N, Dieppois, B, Hannah, DM, Lavers, DA, Fossa, M, Laignel, B & Debret, M

Original citation & hyperlink:
Massei, N, Dieppois, B, Hannah, DM, Lavers, DA, Fossa, M, Laignel, B & Debret, M 2017, 'Multi-time-scale hydroclimate dynamics of a regional watershed and links to large-scale atmospheric circulation: Application to the Seine river catchment, France' *Journal of Hydrology*, vol 546, no. March 2017, pp. 262-275
https://dx.doi.org/10.1016/j.jhydrol.2017.01.008

DOI 10.1016/j.jhydrol.2017.01.008
ISSN 0022-1694
ESSN 1879-2707

Publisher: Elsevier

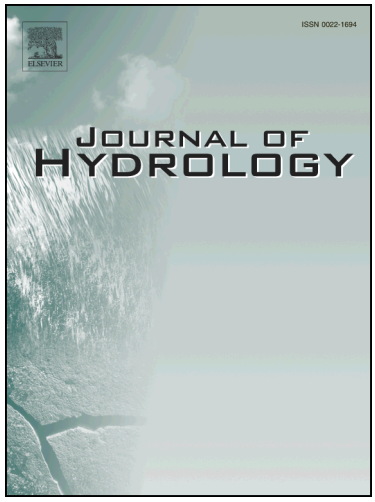

Research papers

Multi-time-scale hydroclimate dynamics of a regional watershed and links to large-scale atmospheric circulation: Application to the Seine river catchment, France

N. Massei, B. Dieppois, D.M. Hannah, D.A. Lavers, M. Fossa, B. Laignel, M. Debret

PII: S0022-1694(17)30009-4
DOI: http://dx.doi.org/10.1016/j.jhydrol.2017.01.008
Reference: HYDROL 21747

To appear in: *Journal of Hydrology*

Received Date: 21 July 2016
Revised Date: 15 November 2016
Accepted Date: 7 January 2017

Please cite this article as: Massei, N., Dieppois, B., Hannah, D.M., Lavers, D.A., Fossa, M., Laignel, B., Debret, M., Multi-time-scale hydroclimate dynamics of a regional watershed and links to large-scale atmospheric circulation: Application to the Seine river catchment, France, *Journal of Hydrology* (2017), doi: http://dx.doi.org/10.1016/j.jhydrol.2017.01.008

MULTI-TIME-SCALE HYDROCLIMATE DYNAMICS OF A REGIONAL WATERSHED AND LINKS TO LARGE-SCALE ATMOSPHERIC CIRCULATION: APPLICATION TO THE SEINE RIVER CATCHMENT, FRANCE

MASSEI N. [1*], DIEPPOIS B. [2,3,4], HANNAH D.M. [5], LAVERS D.A. [6], FOSSA M. [1], LAIGNEL B. [1] & DEBRET M. [1]

* corresponding author: nicolas.massei@univ-rouen.fr

[1] Normandie Univ, UNIROUEN, UNICAEN, CNRS, M2C, 76000 Rouen, France

[2] Department of Oceanography, MARE Institute, University of Cape Town, Cape Town, RSA

[3] Centre for Agroecology, Water and Resilience, Coventry University, Coventry, UK

[4] African Climate & Development Initiative, University of Cape Town, Cape Town, RSA

[5] School of Geography, Earth and Environmental Sciences, University of Birmingham, Edgbaston, Birmingham, B15 2TT, UK.

[6] European Centre for Medium-Range Weather Forecasts, Reading, UK

ABSTRACT

In the present context of global changes, considerable efforts have been deployed by the hydrological scientific community to improve our understanding of the impacts of climate fluctuations on water resources. Both observational and modeling studies have been extensively employed to characterize hydrological changes and trends, assess the impact of climate variability or provide future scenarios of water resources. In the aim of a better understanding of hydrological

changes, it is of crucial importance to determine how and to what extent trends and long-term oscillations detectable in hydrological variables are linked to global climate oscillations.

In this work, we develop an approach associating correlation between large and local scales, empirical statistical downscaling and wavelet multiresolution decomposition of monthly precipitation and streamflow over the Seine river watershed, and the North Atlantic sea level pressure (SLP) in order to gain additional insights on the atmospheric patterns associated with the regional hydrology. We hypothesized that: i) atmospheric patterns may change according to the different temporal wavelengths defining the variability of the signals; and ii) definition of those hydrological/circulation relationships for each temporal wavelength may improve the determination of large-scale predictors of local variations.

The results showed that the links between large and local scales were not necessarily constant according to time-scale (i.e. for the different frequencies characterizing the signals), resulting in changing spatial patterns across scales. This was then taken into account by developing an empirical statistical downscaling (ESD) modeling approach, which integrated discrete wavelet multiresolution analysis for reconstructing monthly regional hydrometeorological processes (predictand: precipitation and streamflow on the Seine river catchment) based on a large-scale predictor (SLP over the Euro-Atlantic sector). This approach basically consisted in three steps: 1- decomposing large-scale climate and hydrological signals (SLP field, precipitation or streamflow) using discrete wavelet multiresolution analysis, 2- generating a statistical downscaling model per time-scale, 3- summing up all scale-dependent models in order to obtain a final reconstruction of the predictand. The results obtained revealed a significant improvement of the reconstructions for both precipitation and streamflow when using the multiresolution ESD model instead of basic ESD. In particular, the multiresolution ESD model handled very well the significant changes in variance through time observed in either precipitation or streamflow. For instance, the post-1980 period, which had been

characterized by particularly high amplitudes in interannual-to-interdecadal variability associated with alternating flood and extremely low-flow/drought periods (e.g., winter/spring 2001, summer 2003), could not be reconstructed without integrating wavelet multiresolution analysis into the model. In accordance with previous studies, the wavelet components detected in SLP, precipitation and streamflow on interannual to interdecadal time-scales could be interpreted in terms of influence of the Gulf-Stream oceanic front on atmospheric circulation.

1. INTRODUCTION

In the present context of global change, considerable efforts have been deployed by the hydrological scientific community to improve our understanding of the impacts of climate fluctuations on water resources (Cloke & Hannah, 2011). Both observational and modeling studies have been employed extensively to characterize hydrological changes, variability and trends (Hannah et al., 2011; Wilson et al, 2013), which appears of primary importance when the question arises of disentangling "natural" and "human-induced" long-term hydrological variations and trends. For instance, streamflow records for the world's major rivers show large decadal to multidecadal fluctuations, with small secular trends for most rivers (Cluis and Laberge, 2001; Lammers et al., 2001; Mauget, 2003; Pekarova et al., 2003; Labat et al., 2004; Giuntoli et al., 2013), which are important to be considered in developing new future scenarios of water resources (e.g. Prudhomme et al., 2014). In addition to identifying and characterizing short- to long-term hydrological variations, improving the understanding of processes driving such changes is of crucial importance in order to determine, in particular, to what extent trends and long-term oscillations in hydrological variables are linked to large-scale climate variability. As mentioned in Laizé et al. (2014), this is vital to improve the skills of hydrological predictions, and prediction of the water cycle.

In Europe, several studies have focused on the investigation of trends and low-frequency variability in hydrological variables (Stahl et al., 2010; Gudmunsson et al., 2011; Kingston et al, 2011). Precipitation over northern Europe experienced upward trends ranging between 6 and 8% from 1900 to 2005 (Trenberth et al., 2007), and these trends are expected to persist over the 21st century (Christensen et al., 2007). Investigating low-frequency variability in streamflow at the pan-European scale, Gudmunsson et al. (2011) showed the existence of long-term oscillations originating from large-scale climate variations, the amplitude of which depended strongly on local watershed physical characteristics. Potential relationships of such low-frequency variability in European streamflow and large scale climate variations have been explored using climate indices, such as the North-Atlantic Oscillation (NAO) (Kiely, 1999; Massei et al., 2007, 2010; Mares et al., 2002; Trigo et al., 2004; Angulo-Martinez and Begueria, 2012; Kingston et al., 2006; Giuntoli et al., 2013; Fritier et al., 2012; Dieppois et al. 2013, 2016). The NAO is considered as a particularly relevant climate indicator over the North Atlantic-Europe sector because changes in NAO phases produce large changes in the mean wind speed and directions, redistributing heat and moisture fluxes from the Atlantic to Europe (Hurrell, 1995; Cassou et al., 2004; Hurrell and Deser, 2009). However, the links between NAO regimes (positive and negative NAO) and European hydroclimate are complex, as it is not constant over time and show seasonal as well as long-term temporal non-stationarity related to the position of NAO poles (Slonosky and Yiou, 2002; Raible et al., 2006; Fritier et al., 2012; Lehner et al., 2012; Dieppois et al., 2016). This is consistent with the conclusions drawn by some authors who pointed out that those circulation indices would likely constitute poor large-scale predictors of local hydrological variations as they do not necessarily capture the most consistent atmospheric pattern linked to observed hydrological variation (e.g., Lavers et al., 2010a, 2010b). In France, Giuntoli et al. (2013) pointed out the difficulty to use climate indices (NAO, AMO/Atlantic Multidecadal Oscillation) as hydrological predictors. They nevertheless highlight better skills in predicting low-flow using weather patterns than using climate

indices such as NAO or AMO. Yet, by studying the links between hydrological variations (precipitation and streamflow) on the Seine river watershed and the NAO index using spectral and multiresolution time series analyses, Massei et al. (2010) and Massei and Fournier (2012) demonstrated significant correlation at some interannual and interdacadal time scales, and thus highlighted potential skills for hydrological predictions. Boé and Habets (2014) and Dieppois et al. (2016) highlighted the critical role of multidecadal climate variability on hydrological variations over France. Such multidecadal fluctuations in hydrological variations are indeed likely to strongly modulate trend, as it has been the case from the mid-19th century in winter and spring (Dieppois et al., 2016). This also holds for the coming decades, as at the regional and local scales, internal climate variability is likely to be as important as anthropogenic climate changes in the middle and high latitudes (Deser et al., 2012, 2014). Therefore, to improve our prediction skills of hydrological variations, it appears of particular interest to determine the way hydrological and climatic signals oscillate together at different time-scales, and to develop new statistical downscaling strategies accounting for those low-frequency ($\geq$ 2 year up to multidecadal) time-scales of variability.

To address the above research gaps, this study builds on some previous work, which investigated high- to low-frequency oscillations in northern France/central England precipitation and streamflow (Fritier et al., 2012; Massei et al., 2010; Massei and Fournier, 2012; Dieppois et al., 2013; Dieppois et al., 2016). Here, we tested the potential value-added of combining discrete wavelet multiresolution decomposition and statistical downscaling for studying, understanding and predicting the links between precipitation or streamflow over the Seine river watershed with atmospheric circulation patterns using sea level pressure (SLP) in the Euro-Atlantic sector. We aimed at gaining new insights into the atmospheric patterns driving regional hydrology. In particular, the following hypotheses were tested: (1) do atmospheric patterns related to local hydrology remain unchanged whatever the different characteristic frequencies over which atmospheric and hydrological signals oscillate? (2) would accounting for time-scale-dependent

characteristics of the large-scale circulation/local-scale hydrological variation relationships help improving the results of empirical statistical downscaling models of local or regional hydrology?

2. DATA AND METHODS

2.1 HYDRO-CLIMATOLOGICAL DATA

The Seine is one of the main French rivers (Fig.1), with precipitation regime in the area is typically of pluvio-oceanic type. Its catchment area is ~78 000 km2 and comprises almost one third of the French population. With large regions devoted to agriculture and many large urban zones including Paris, it is heavily impacted by human activities. As a result such catchments are not classically considered as the most appropriate for investigating the linkages between hydrological and large-scale climate variability (Hannah et al., 2011). However, improving our understanding of such links for such basins appears crucial precisely because a huge amount of the population of the country depends on its water resources. As in many rivers in northern France, the Seine is sustained by major groundwater aquifers. In the case of the Seine River, these aquifers develop within the wide Paris basin syncline, which comprises several hydrogeological units, either confined or unconfined.

The Climatic Research Unit (CRU) data-set was used to estimate precipitation data. The CRU TS 3.21 rainfall field was produced on a 0.5°×0.5° grid and derived from monthly rainfall provided by about 4,000 weather stations distributed around the world over the last centuries (http://catalogue.ceda.ac.uk/uuid/3f8944800cc48e1cbc29a5ee12d8542d for more explanations for this dataset). A regional precipitation index between January 1950 and December 2007 was constructed by averaging the values over an irregular region matching the Seine river watershed boundaries. Seine river streamflow data was provided by the French hydrological database Banque HYDRO (http://www.hydro.eaufrance.fr/). River flow time series between January 1950 and

December 2007 was available on a daily time-step but aggregated monthly, as this study was designed for investigation of long-term hydrological variability.

National Center for Environmental Prediction/National Center for Atmospheric Research-1 (NCEP/NCAR-1) reanalysis (1948–Present; Kalnay et al., 1996) was used to infer monthly North Atlantic atmospheric dynamics over the North Atlantic region (75°W-35°E and 15°-75°N), with a 2.5°×2.5° horizontal resolution (i.e., 1125 grid-points). Only mean sea-level pressure (SLP), which is a good indicator of regional to local hydroclimatic conditions in the mid- to high latitude, was used between January 1950 and December 2007.

In the subsequent parts of the analysis SLP will be referred to as to "large-scale" variable, while precipitation and streamflow will be referred to as "local-scale" variables.

2.2 METHODS

The general approach developed herein intends to: (1) identify the main time-scales of variability of SLP, precipitation and streamflow time series; and (2) characterize the spatial patterns of the relationships between the large-scale climate field (SLP over the North Atlantic) and local-scale hydro-climatological signals (precipitation and streamflow in the Seine river watershed) according to these time-scales, *i.e.*, identify potential predictors; (3) examine the ability of time-scale decomposition in predicting slow fluctuations of local hydroclimatology by empirical statistical downscaling.

Continuous wavelet transform was used as a preliminary step for visualizing the spectral content of precipitation and steamflow signals. Then, all hydrological and SLP field signals were processed using wavelet multiresolution analysis and synthesis in order to obtain the high- to low-frequency components contained in each signal. Multiresolution decomposition results were then used for generating scale-dependent SLP composite maps based on hydrological variations, which allowed

exploring the SLP patterns related to hydrology for different time-scales. Finally, we integrated the wavelet multiresolution framework into an empirical statistical downscaling approach in order to test whether accounting for the different time-scales over which hydrological and atmospheric climate field time series vary would help improving statistical downscaling models.

First, monthly precipitation and streamflow time series were analyzed using continuous wavelet transform (CWT), which allowed a first exploration of the spectral content of the hydrological signals. Typical scales of variability of each time series were thus detected and a first comparison of time-scale patterns identified in each variable was undertaken. CWT is a well-known method that has been used over the past decade for data analysis in hydrology, geophysics and environmental sciences (Torrence and Compo 1998; Labat, 2005; Sang, 2013). For more technical details, a very rich literature on the application of wavelet analysis to geophysical time series is available; for instance, the paper by Torrence and Compo (1998) provides a very good overview of continuous wavelet techniques and their theoretical background. The continuous wavelet transform produces a time-scale (or time-period with the meaning of Fourier transform) contour diagram on which time is indicated on the x-axis, period or scale on the y-axis and amplitude (or variance, or power, etc.) on the z-axis.

Second, all monthly time series (SLP gridded-data, precipitation and streamflow) were decomposed by wavelet multiresolution analysis into different internal components corresponding to different time-scales. Briefly, multiresolution analysis consists in the iterative filtering of the time series using a series of low-pass and high-pass filters which eventually produce one high-frequency "rough" component called "wavelet detail" and one lower-frequency "coarse" component called "smooth" or "approximation". The smooth produced at each scale is then subsequently decomposed into a second wavelet detail and a second smooth, the latter to be decomposed again in the same way until one last smooth remain that will no longer be decomposed. Summing up all wavelet

details and the last smooth (i.e. the lowest-frequency component) gives back the original signal. We will not discuss here the mathematical basis of multiresolution analysis, which can be easily accessed in the very rich literature on the topic (see for instance Labat et al., 2000): it is only needed to keep mind that one given signal can be separated into a relatively small number of wavelet components from high to low frequencies that altogether explain the variability of the signal, as this will be illustrated later using precipitation and streamflow time series. Daubechies least asymmetric wavelet and scaling functions of order 8, *i.e.* comprising 8 coefficients have been chosen here: this choice seemed to be well-suited to the relative smoothness of monthly signals. Conversely, order 2 filters (resulting in the well-known Haar wavelet) are usually better suited for analyzing and processing coarser signals, while higher order filters are usually suitable when signals are smoother. Precipitation, streamflow, as well as each of the 1125 grid-points of the monthly SLP field were decomposed by wavelet multiresolution analysis, resulting in 9 wavelet details plus 1 smooth in each case. As a result, the process ended up with 9 wavelet details plus 1 smooth for precipitation, for streamflow, as well as for the SLP field (i.e., for each of the 1125 grid-points).

The next step consisted of exploring the spatial patterns associated to the precipitation/SLP and streamflow/SLP relationships to gain insights into potential changes according to time-scale, since natural geophysical signals can behave very differently on different time-scales: does SLP predictor of local hydrological variability remain constant in terms of spatial structure whatever the time-scale of oscillation considered in both hydrological variables and SLP field? Such a hypothesis was tested:

1- by generating one SLP composite map for each wavelet scale. At any given time-scale, a SLP composite map was constructed by taking the values of the SLP wavelet component at this scale during periods of high-amplitude (*i.e.* below and above 0.5 standard deviation [SD]) of the wavelet component of precipitation and streamflow at the same scale. Two sets of North Atlantic SLP time-

series were then produced at each time-scale, one corresponding to SLP values when the local hydrological variable (river flow or precipitation) values were higher than 0.5 SD (SLP+), the other when hydrological variable values was lower than -0.5 SD (SLP-). The SLP composite map based on either precipitation or streamflow variations maps the difference between the SLP+ and SLP- time-series. The statistical significance of this difference is estimated by testing the difference in mean of the two sets using a Student's t-test at p=0.9. The number of degrees of freedom had to be adjusted according to the wavelet scale by recalculating the "effective" sample size N' from the actual sample size N according to the first-order autocorrelation coefficient AR[1] of each of the two SLP time-series (Mitchell et al., 1966), i.e.:

$$N' = N ((1-AR[1]) / (1+AR[1])) \quad (1)$$

This was necessary in order to account for different autocorrelation in the time-series according to the different wavelet details extracted: lower-frequency wavelet details are affected by higher autocorrelation than higher-frequency ones and the subsequent number of degrees of freedom should decrease when frequency gets lower.

2- by integrating wavelet multiresolution decomposition into an empirical statistical downscaling (ESD) process. ESD modeling strategy was based on multiple linear regression of the local variables on empirical orthogonal functions (EOFs) of atmospheric fields (Benestad, 2011) on a monthly basis. The so-called multiresolution ESD approach consisted of: (1) deriving one statistical downscaling model for each wavelet decomposition level (i.e. for each wavelet detail/each time-scale) of the atmospheric field and local hydrometeorological variables; (2) summing up all models at the end of the process given orthogonality of the wavelet decomposition technique used. The resulting multiresolution ESD model was expected to deal better with the characteristics of the relationships between the large and local spatial scales at each time-scale.

Data analyses were undertaken using R packages biwavelet (Gouhier and Grinsted, 2012), wmtsa (Constantine and Percival, 2016), and clim.pact (Benestad, 2011).

3. RESULTS

3.1. CHARACTERISTIC TIME-SCALES OF PRECIPITATION AND STREAMFLOW OSCILLATIONS AND TRENDS

CWT spectra of precipitation and streamflow display energetic peaks at several time scales (Fig. 2A, B). No annual variability was detected in precipitation, contrary to streamflow which displayed high power around 1 year almost constant through time as a result of the impact of temperature/evapotranspiration seasonality. At time-scales greater than 2 years, very similar time-scale patterns are observed in both precipitation and streamflow. In particular, energetic peaks at ~5-10 year and ~18 year periods were observed after 1970s/80s showing increasing variance in precipitation and streamflow at these scales as already shown by Massei et al. (2010) et Fritier et al. (2012)..

Multiresolution analysis was applied to local hydrological and climate field time series to achieve full time-scale decomposition of each signal. The process resulted in separation of 10 components, *i.e.*, 9 wavelet details and 1 smooth for each signal (Figs. 3 and 4). Variability of precipitation and streamflow could then be explored across different time-scales. Precipitation was clearly dominated by high-frequency variability (D1/~3 months) and D2/~6-months), explaining 72% of total precipitation energy (Table 1). On the other hand, annual and lower-frequency components, *i.e.*, between D3 (annual cycle) and D9 (58-yr) explained 28% of total precipitation energy (Table 1). As previously noticed on streamflow CWT, the annual cycle was much more pronounced in streamflow variability, explaining 45.5% of total energy (D3; Fig.4 and Table 2). Both precipitation and streamflow exhibited similar oscillatory components on interannual to interdecadal time scales

(D4/1.5–1.9-yr to D9/58-yr in Fig.3 and 4), which were not easy to detect by simple visual inspection of the precipitation and streamflow time-series (gray time-series in the background in figures 3 and 4). Details D8 (29 years) and D9 (58 years) correspond, respectively, to a long-term oscillation and a trend of about half the length up to the total length of the time series. The last component (smooth S9) was constant in precipitation and streamflow and corresponded to the mean of each time series, demonstrating all varying components had been successfully extracted. The interannual spectral peaks of periods ~5-10 yr and ~18 yr identified previously on the precipitation CWT spectrum were clearly captured by multiresolution analysis as details D6 and D7. As a whole, low-frequency variability (> oscillations greater than 1 year) explained 14.9% and 31.1% of total energy for precipitation and streamflow, respectively.

3.2. RELATIONSHIP WITH NORTH ATLANTIC CIRCULATION PATTERNS

SLP composite maps were generated based on precipitation and streamflow variations in the Seine watershed (Figs. 5 and 6). Seven composite maps were generated based for both precipitation and streamflow variations, corresponding to time-scales ranging from ~0.2 yr to ~19.3 yr. Composites were not calculated for D8 (29-yr) and S9 (58-yr), as fluctuations on such time-scales only corresponded to very low-frequency variability of about the length or half the length of the time series (visible in Figs. 3 and 4), because they only explained a very low contribution to total energy (Tables 1 and 2), and because they were not statistically significant as shown by CWT (Fig.2A and B). Hence, such maps reflect the magnitude and sign of the co-variation between precipitation/streamflow and the SLP field. The identified regions describe spatial patterns that display significant changes according to the time-scale considered in terms of spatial extent, location of high- and low-pressure regions.

At each time-scale, SLP composite anomalies impacting precipitation variability show high-pressure anomalies over the northern North Atlantic as well as low-pressure anomalies centered on

the English Channel and the North Sea (Fig.5). This is associated with cyclonic circulation over northwestern Europe, which, south of 50°N, is likely to increase westerly moisture fluxes from the Atlantic to the continent, and to the Seine river watershed. At time-scales of 3.2 years (D5) and 19.3 years (D7), dipolar SLP anomalies between the northern North Atlantic and the subtropical Atlantic to northwestern Europe are increasingly spatially coherent, and are quite reminiscent of SLP anomalies associated with a negative NAO. This should also be associated with increasing southwesterlies from the Atlantic to the Seine river watershed, while westerlies should be weakening in the northern North Atlantic. SLP composite anomalies related to streamflow variability are quite similar to those associated with precipitation. Differences between SLP composite anomalies based on precipitation and streamflow are mainly observed for short time-scales (D1/2-months to D3/1 year). For the shortest time-scales lower than 1 year, differences are very likely due to the filtering effect of the watershed as a result of the large size of the catchment and of a high contribution of ground water flow, which on the regional scale smoothes out higher-frequency variations (El Janyani et al., 2012; Slimani et al., 2009). Significant differences observed for the 1-yr time-scale would be likely related to the seasonal influence of temperature on streamflow *via* evapotranspiration, while annual cycle is only poorly expressed in precipitation in the study area. It might then not be very physically consistent to consider and interpret time-scales lower than or equal to 1 year for streamflow-based composites. On the other hand, low-frequency variations are captured quite similarly in both precipitation and streamflow. Such a result was totally expected insomuch as precipitation and streamflow wavelet details at such large time-scales already displayed nearly identical variabilities (see for instance details D5 to D9 in figures 3 and 4). However, using either precipitation or streamflow variations, the wavelet-based composite analysis highlighted that the spatial extent of atmospheric patterns were not strictly similar according to the different time-scales of hydro-climatic variability. This suggests that the different scales over which

local hydro-climatic processes vary, may not be necessarily related to the same type of atmospheric circulation process.

4. TIME-SCALE-DEPENDENT STATISTICAL DOWNSCALING

10 components were obtained from the wavelet decomposition (*i.e.* 9 wavelet details plus one smooth) of each of the 3 variables (SLP field, the precipitation and streamflow time series). 10 statistical downscaling models for both precipitation and streamflow were then derived, *i.e.* one for each scale. Model parametrization then becomes (time-)scale-dependent. The ESD modeling is based on a multiple regression on SLP EOFs. The number of EOFs supporting the model had to be determined as following. This number should be high enough to ensure that most of the consistent large-scale patterns explaining local-scale variability are accounted for. However, using too many EOFs may result in overfitting, and then lead to inconsistent physical interpretation as too much noise enters the modeling process. From the amount of variance explained by each principal component, it seemed that only the first 8 EOFs of the SLP field are needed in the model (all higher-order components would explain < 5% of total variance).

At each scale, the model resulted in a map of regression coefficients corresponding to the SLP patterns (*i.e.* the predictor), and in a modeled time series of either precipitation or streamflow (i.e. the predictand). Figures 7 displays the SLP predictor patterns for precipitation, i.e. the map of multiple regression coefficients for the precipitation model at each time-scale. A careful visual inspection of how the large-scale predictor patterns compare with precipitation-based composite maps (Figs. 5) revealed similar spatial features for all time-scales, which confirms that the modeled emergent patterns of the large-scale/local-scale relationships are robust. Regression coefficient maps were generated in exactly the same way for streamflow (not shown); the spatial patterns

described by the multiple regression model also matched quite well streamflow-based composite maps.

The quality of monthly precipitation and streamflow reconstructions obtained with ESD and multiresolution ESD was assessed using the Nash-Sutcliffe efficiency criterion (NSE) and coefficient of determination (R^2). NSE and R^2 coefficients showed improvement of the ESD model for both precipitation and streamflow when wavelet multiresolution decomposition was used. For instance, NSE was 0.48 for the monthly precipitation ESD model (Fig.8B), whereas it reached 0.54 (Fig.8A) for the multiresolution ESD model (resp. 0.47 and 0.54 for streamflow, not shown). Comparison of continuous wavelet spectra of observed precipitation (Fig.2A), ESD model (Fig. 9A) and multiresolution ESD model (Fig. 9B) indicated that most of the improvement provided by multiresolution ESD involved a better simulation of interannual to interdecadal time-scales, which the ESD model was not able to reproduce. The continuous wavelet spectrum of the multiresolution ESD simulation (Fig.9B) clearly displays the same time-frequency structures as those of observed precipitation CWT (Fig.2A) for periods higher than 4 years.

Owing to the capability of wavelet analysis to capture both high and low-fequency variabilities, the value-added of multiresolution ESD over ESD is getting clearer when monthly observed and downscaled time series are aggregated on an annual time step: the multiresolution ESD model performed well in reproducing long-term variations, whereas the ESD model completely failed in capturing low-frequency variations, especially for streamflow (Fig.10 A and B). Predicting capabilities of the multiresolution ESD approach were tested for a 9-yr lead time (Fig. 10C), as such a duration allows for taking into account high-amplitude interannual variations characterizing hydrological variations in precipitation, river flow and ground water levels within the study area (El Janyani et al., 2012; Massei et al., 2010; Slimani et al., 2009). The multiresolution ESD model was successful in predicting observed high precipitation amounts of the late 90's-early 2000 period

(connected points). On the other hand, the ESD model was not able to catch the high amplitudes of observed precipitation during the same period.

5. DISCUSSION

From the results we can conclude that slightly different atmospheric patterns could be related to precipitation or streamflow variations according to the time scale considered, which characterizes the non-linear nature of the large-scale circulation/local-scale hydrology connections. Lavers et al. (2015) already highlighted the existence of such non-linear characteristics. Their results suggested that different sequences (order, spacing in time) of atmospheric and water vapour transport patterns during the past months prior to streamflow or ground water level observations could be observed and potentially lead to similar high/low streamflow or ground water levels. Our own results provided enlightenment on the origin of such non-linear characteristics of the relationships between large-scale and local-scale: at any given time a high (or low) precipitation or streamflow may be related to different combinations of several, not necessarily similar oscillating atmospheric patterns of different time-scales (*e.g.* either high-amplitude low-frequency with low-amplitude highest frequencies or conversely). The integration of a multiresolution approach into downscaling studies then proves useful for assessing non-linear features of the connections between large-scale climate variability and local-scale hydro-meteorological changes.

Investigating the physical meaning of ~3 months and ~6 months shorter-term oscillations seemed difficult in the context of this study, and should be done through multimodel climate ensemble. However, interannual to interdecadal oscillations had already been highlighted in numerous previous works in the winter months NAO index, baroclinic Rossby waves and North-Atlantic sub-tropical gyre (Terray and Cassou, 2002; Massei et al., 2007; Fritier et al., 2012; Pinault, 2012, as well as many others). While Massei et al. (2007) reported 2.4-yr, 5.4-yr, 7.6-yr, 20.6-yr fluctuations

in the winter NAO, Feliks et al. (2011) found significant oscillatory modes with periods of 2.8-yr, 4.2-yr, and 8.5-yr in both observed NAO index and a NAO atmospheric marine boundary layer simulation forced with SST from a SODA (Simple Ocean Data Analysis) reanalysis: according to Feliks et al. (2011) these atmospheric oscillatory modes in the simulations were found to be induced by the Gulf Stream oceanic front. In addition, in our study, oscillatory components of precipitation and streamflow on sub-annual and 7.2-yr times-scales were associated to SLP patterns that appeared very similar to those found by Lavers et al. (2010) for several January precipitation and streamflow observations in the Great Stour Basin, southeastern England. These patterns were not exactly reminiscent of the NAO, as highlighted by Lavers et al. (2010), with centers of action actually shifted to the North. On the other hand, interannual ~3.2-yr (and to a lesser extent 1.5/1.9-yr) and interdecadal ~19.3-yr components for both precipitation and streamflow revealed a much more spatially extended pattern across the Atlantic with lower SLP roughly following the Gulf Stream front. These components are represented in figure 11 and would then illustrate this part of local-scale precipitation or streamflow variability most directly linked to large-scale oceanic/atmospheric circulation processes. Although SLP was used in this study, it would be interesting to account for other types of potential large-scale climate drivers (different geopotential heights, meridional and zonal wind, atmospheric moisture flux, sea surface temperature, etc.).

We noted that beyond the 1-yr time-scale, the large-scale patterns associated to precipitation and streamflow variations became quite similar in terms of both spatial structures and amplitude, even if river flow was not naturalized before conducting the analysis. One main source of anthropogenic influence on Seine river is due to the presence of 4 large reservoirs at the headwaters of the catchment, along with water abstraction for agriculture. It is interesting to notice that the existence of such impacts does not prevent river discharge from recording low-frequency large-scale atmospheric influence quite similarly as precipitation, whereas the watershed would normally not be tagged as climate-sensitive. Of course, additional physics-based research would be needed in

order to assess how both natural (infiltration, ground water flow and discharge) and anthropogenic (water abstraction, reservoirs) physical processes impact the amplitude of low-frequency streamflow variations originating from climate variability.

From a methodological standpoint, the multiresolution ESD approach seemed fairly robust so far: for instance, the results did not seem to be highly sensitive to the type of wavelet/scale functions used. 10 least asymetric daubechies scale and associated wavelet functions with 2, 4, 6, 8, 10, 12, 14, 16 18 and 20 coefficients were tested: the shape of the spatial patterns (not shown) never displayed significant changes that may lead to different physical interpretations. As a consequence, no significant differences could be notice for the 10 different multiresolution ESD models (Fig. 12). Yet, the method would still need to be more deeply explored. For instance, the method depends on the length of the time-series available, which controls the number of wavelet components and associated time-scales extracted: the sensitivity of the multiresolution downscaling approach to this characteristics (what is actually gained when the time series used are short, e.g., less than two decades?) would also need deeper investigation.

6. CONCLUSION

In order to account for the non-linearity of hydro-climatological processes, a multiresolution approach was applied to investigate the scale dependence of the connections between local-scale hydrology and large-scale atmospheric circulation characteristics. Since climatological and hydrometeorological signals display variability and oscillations on different time-scales, we hypothesized that large-scale/local-scale links may not be necessarily constant across time scales. Our results emphasized that the large-scale patterns associated to the different oscillating modes of local-scale precipitation and streamflow were not the same according to time-scale, which is typical of a non-linear behavior of such relationships. SLP patterns found were not necessarily similar to

pre-established weather regimes such as the NAO. The corresponding time-scales in SLP and local hydrological variables proved not only statistically significant, but might also be related to some physical mechanisms linked to North-Atlantic oceanic/atmospheric circulation coupling, which were found to oscillate at the same time-scales as highlighted by other studies. Implementation of those findings in an empirical statistical downscaling model resulted in a much better simulation of local-scale variability, in particular for frequency greater than 2 years. The so-called multiresolution ESD downscaling approach thus proved useful in the aim of reproducing the different oscillations and trends that exist in hydrological variables. Validation over a 9-yr lead time provided satisfactory results, as the downscaling model successfully simulated high hydro-climatic conditions whereas the simple ESD model was not able to handle such variability. One next possible step would be the application of the multiresolution ESD approach for investigating the large-scale/local-scale relationships per season or per month of the year, which may be affected by different long-term interannual/interdecadal behaviors. Finally, the possibility of using the multiresolution ESD approach for reconstruction of hydrological time-series back in time would also deserve thorough investigation.

ACKNOWLEDGEMENTS

The authors are grateful to the Seine-Aval Upper Normandy regional scientific programme, as well as the French National Agency for Water and Aquatic Environments ONEMA (Office National de l'Eau et des Milieux Aquatiques) for financial support. The authors would also like to thank two anonymous reviewers for their thoughtful comments that definitely helped improving the paper.

REFERENCES

Angulo-Martínez, M., & Beguería, S. (2012). Trends in rainfall erosivity in NE Spain at annual, seasonal and daily scales, 1955–2006. Hydrology and Earth System Sciences, 16(10), 3551–3559. http://doi.org/10.5194/hess-16-3551-2012

Benestad, R.E. (2011). clim.pact: Climate analysis and empirical-statistical downscaling (ESD) package for monthly and daily data. R package version 2.3-10 (now maintained in CRAN as package “ESD”).

Boé, J., & Habets, F. (2013). Multi-decadal river flows variations in France. Hydrology and Earth System Sciences Discussions, 10(9), 11861–11900. http://doi.org/10.5194/hessd-10-11861-2013

Cassou, C., Terray, L., Hurrell, J. W., & Deser, C. (2004). North Atlantic winter climate regimes: Spatial asymmetry, stationarity with time, and oceanic forcing. Journal of Climate, 17(5), 1055–1068.

Christensen, N. S., & Lettenmaier, D. P. (2007). A multimodel ensemble approach to assessment of climate change impacts on the hydrology and water resources of the Colorado River Basin, 1417–1434.

Cloke, H. L., & Hannah, D. M. (2011). Large-scale hydrology: Advances in understanding processes, dynamics and models from beyond river basin to global scale. Hydrological Processes, 25(7), 991–995. http://doi.org/10.1002/hyp.8059

Cluis, D., & Laberge, C. (2001). Climate Change and Trend Detection in Selected Rivers within the Asia-Pacific Region. Water International, 26(3), 411–424. http://doi.org/10.1080/02508060108686933

Constantine, W., & Percival, D. (2016). wmtsa: Wavelet Methods for Time Series Analysis. R package version 2.0-1. https://CRAN.R-project.org/package=wmtsa

Deser, C., Phillips, A., Bourdette, V., & Teng, H. (2012). Uncertainty in climate change projections: The role of internal variability. Climate Dynamics, 38(3-4), 527–546. http://doi.org/10.1007/s00382-010-0977-x

Deser, C., Phillips, A. S., Alexander, M. A., & Smoliak, B. V. (2014). Projecting North American climate over the next 50 years: Uncertainty due to internal variability. Journal of Climate, 27(6), 2271–2296. http://doi.org/10.1175/JCLI-D-13-00451.1

Dieppois, B., Durand, A., Fournier, M., & Massei, N. (2013). Links between multidecadal and interdecadal climatic oscillations in the North Atlantic and regional climate variability of northern France and England since the 17th. Journal of Geophysical Research: Atmospheres, 118, 4359–4372. http://doi.org/10.1002/jgrd.50392

Dieppois, B., Lawler, D. M., Slonosky, V., Massei, N., Bigot, S., Fournier, M., & Durand, A. (2016). Multidecadal climate variability over northern France during the past 500 years and its relation to large-scale atmospheric circulation. International Journal of Climatology, n/a–n/a. http://doi.org/10.1002/joc.4660

Feliks, Y., Ghil, M., & Robertson, A. W. (2011). The atmospheric circulation over the North Atlantic as induced by the SST field. Journal of Climate, 24(2), 522–542. http://doi.org/10.1175/2010JCLI3859.1

Fritier, N., Massei, N., Laignel, B., Durand, A., Dieppois, B., & Deloffre, J. (2012). Links between NAO fluctuations and inter-annual variability of winter-months precipitation in the Seine River watershed (north-western France). Comptes Rendus Geoscience, 344(8), 396–405. http://doi.org/10.1016/j.crte.2012.07.004

Giuntoli, I., Renard, B., Vidal, J.-P., & Bard, A. (2013). Low flows in France and their relationship to large-scale climate indices. Journal of Hydrology, 482, 105–118. http://doi.org/10.1016/j.jhydrol.2012.12.038

Gouhier, T.C., & Grinsted, A. (2012). biwavelet: Conduct univariate and bivariate wavelet analyses. R package version 0.12. http://CRAN.R-project.org/package=biwavelet

Gudmundsson, L., Tallaksen, L. M., Stahl, K., & Fleig, A. K. (2011). Low-frequency variability of European runoff. Hydrology and Earth System Sciences, 15(9), 2853–2869. http://doi.org/10.5194/hess-15-2853-2011

Hannah, D. M., Demuth, S., van Lanen, H. A. J., Looser, U., Prudhomme, C., Rees, G., … Tallaksen, L. M. (2011). Large-scale river flow archives: Importance, current status and future needs. Hydrological Processes, 25(7), 1191–1200. http://doi.org/10.1002/hyp.7794

Hurrell, J. W. (1995). Decadal trends in the north atlantic oscillation: regional temperatures and precipitation. Science (New York, N.Y.), 269(5224), 676–679.

Hurrell, J. W., & Deser, C. (2009). North Atlantic climate variability: The role of the North Atlantic Oscillation. Journal of Marine Systems, 78(1), 28–41. http://doi.org/10.1016/j.jmarsys.2008.11.026

El Janyani, S., Massei, N., Dupont, J., & Fournier, M. (2012). Journal of Hydrology, 465, 485–493.

Kalnay, E., Kanamitsu, M., Kistler, R., Collins, W., Deaven, D., Gandin, L., … Joseph, D. (1996). The NCEP/NCAR 40-year reanalysis project. Bulletin of the American Meteorological Society. http://doi.org/10.1175/1520-0477(1996)077<0437:TNYRP>2.0.CO;2

Kiely, G. (1999). Climate change in Ireland from precipitation and streamflow observations. Advances in Water Resources, 23(2), 141–151. http://doi.org/10.1016/S0309-1708(99)00018-4

Kingston, D. G., Hannah, D. M., Lawler, D. M., & Mcgregor, G. R. (2011). Regional classification, variability, and trends of northern North Atlantic river flow. Hydrological Processes, 25(7), 1021–1033. http://doi.org/10.1002/hyp.7655

Kingston, D. G., McGregor, G. R., Hannah, D. M., & Lawler, D. M. (2006). River flow teleconnections across the northern North Atlantic region. Geophysical Research Letters, 33(14), L14705. http://doi.org/10.1029/2006GL026574

Labat, D. (2005). Recent advances in wavelet analyses: Part 1. A review of concepts. Journal of Hydrology, 314(1-4), 275–288. http://doi.org/10.1016/j.jhydrol.2005.04.003

Labat, D., Ababou, R., & Mangin, A. (2000). Rainfall-runoff relations for karstic springs. Part II: Continuous wavelet and discrete orthogonal multiresolution analyses. Journal of Hydrology, 238(3-4), 149–178. http://doi.org/10.1016/S0022-1694(00)00322-X

Labat, D., Goddéris, Y., Probst, J. L., & Guyot, J. L. (2004). Evidence for global runoff increase related to climate warming. Advances in Water Resources, 27(6), 631–642. http://doi.org/10.1016/j.advwatres.2004.02.020

Laizé, C. L. R., Acreman, M. C., Schneider, C., Dunbar, M. J., Houghton-Carr, H. A., Flörke, M., & Hannah, D. M. (2014). Projected flow alteration and ecological risk for pan-european rivers. River Research and Applications, 30(3), 299–314. http://doi.org/10.1002/rra.2645

Lammers, R. B., Shiklomanov, A. I., Vörösmarty, C. J., Fekete, B. M., & Peterson, B. J. (2001). Assessment of contemporary Arctic river runoff based on observational discharge records. Journal of Geophysical Research, 106, 3321. http://doi.org/10.1029/2000JD900444

Lavers, D. A., Hannah, D. M., & Bradley, C. (2015). Connecting large-scale atmospheric circulation, river flow and groundwater levels in a chalk catchment in southern England. Journal of Hydrology, 523, 179–189. http://doi.org/10.1016/j.jhydrol.2015.01.060

Lavers, D., Prudhomme, C., & Hannah, D. M. (2010a). Large-scale climate, precipitation and British river flows: Identifying hydroclimatological connections and dynamics. Journal of Hydrology, 395(3-4), 242–255. http://doi.org/10.1016/j.jhydrol.2010.10.036

Lavers, D., Prudhomme, C., & Hannah, D. M. (2010b). Large-scale climatic influences on precipitation and discharge for a British river basin. Hydrological Processes, 24(18), 2555–2563. http://doi.org/10.1002/hyp.7668

Lehner, F., Raible, C. C., & Stocker, T. F. (2012). Quaternary Science Reviews, 45, 85–94. http://doi.org/10.1016/j.quascirev.2012.04.025

Mares, I., Mares, C., & Mihailescu, M. (2002). NAO impact on the summer moisture variability across Europe. Physics and Chemistry of the Earth, 27(23-24), 1013–1017. http://doi.org/10.1016/S1474-7065(02)00135-3

Massei, N., Durand, A., Deloffre, J., Dupont, J. P., Valdes, D., & Laignel, B. (2007). Investigating possible links between the North Atlantic Oscillation and rainfall variability in northwestern France over the past 35 years. Journal of Geophysical Research: Atmospheres, 112, 1–10. http://doi.org/10.1029/2005JD007000

Massei, N., & Fournier, M. (2012). Assessing the expression of large-scale climatic fluctuations in the hydrological variability of daily Seine river flow (France) between 1950 and 2008 using Hilbert-Huang Transform. Journal of Hydrology, 448-449, 119–128. http://doi.org/10.1016/j.jhydrol.2012.04.052

Massei, N., Laignel, B., Deloffre, J., Mesquita, J., Motelay, A., Lafite, R., & Durand, A. (2010). Long-term hydrological changes of the Seine River flow (France) and their relation to the North Atlantic Oscillation over the period 1950-2008. International Journal of Climatology, 30(14), 2146–2154.

Mauget, S. A. (2003). Multidecadal regime shifts in U.S. streamflow, precipitation, and temperature at the end of the twentieth century. Journal of Climate, 16(23), 3905–3916. http://doi.org/10.1175/1520-0442(2003)016<3905:MRSIUS>2.0.CO;2

Mitchell, J.M., Jr., Dzerdzeevskii, B., Flohn, H., Hofmeyr, W.L., Lamb, H.H., Rao, K.N., and Wallén, C.C. (1966), Climatic change: Technicall Note No. 79, report of a working group of the Commission for Climatology. WMO No. 195 TP 100: Geneva, Switzerland, World Meteorological Organizaton, 81 p.

Pekárová, P., Miklánek, P., & Pekár, J. (2003). Spatial and temporal runoff oscillation analysis of the main rivers of the world during the 19th-20th centuries. Journal of Hydrology, 274(1-4), 62–79. http://doi.org/10.1016/S0022-1694(02)00397-9

Percival, D.B., & Walden, A.T. (2000). wmtsa : software to book Wavelet Methods for Time Series Analysis, Cambridge University Press.

Pinault, J.-L. (2012). Global warming and rainfall oscillation in the 5–10 yr band in Western Europe and Eastern North America. Climatic Change, 114(3-4), 621–650. http://doi.org/10.1007/s10584-012-0432-6

Prudhomme, C., Giuntoli, I., Robinson, E. L., Clark, D. B., Arnell, N. W., Dankers, R., Fekete, B.M., Franssen, W., Gerten, D., Gosling, S.N., Hagemann, S., Hannah, D.M., Kim, H., Masaki, Y., Satoh, Y., Stacke, T., Wada, Y., Wisser, D. (2014). Hydrological droughts in the 21st century, hotspots and uncertainties from a global multimodel ensemble experiment. Proceedings of the National Academy of Sciences of the United States of America, 111(9), 3262–7. http://doi.org/10.1073/pnas.1222473110

Raible, C. C., Casty, C., Luterbacher, J., Pauling, A., Esper, J., Frank, D. C., … Wanner, H. (2006). Climate variability-observations, reconstructions, and model simulations for the Atlantic-European

and Alpine region from 1500-2100 AD. Climatic Change, 79(1-2), 9–29. http://doi.org/10.1007/s10584-006-9061-2

Sang, Y.-F. (2013). A Review On The Applications Of Wavelet Transform In Hydrology Time Series Analysis. Atmospheric Research, 122, 8–15. http://doi.org/10.1016/j.atmosres.2012.11.003

Slimani, S., Massei, N., Mesquita, J., Valdés, D., Fournier, M., Laignel, B., & Dupont, J.-P. (2009). Combined climatic and geological forcings on the spatio-temporal variability of piezometric levels in the chalk aquifer of Upper Normandy (France) at pluridecennal scale. Hydrogeology Journal, 17(8), 1823–1832. http://doi.org/10.1007/s10040-009-0488-1

Slonosky, V., & Yiou, P. (2002). Does the NAO index represent zonal flow? The influence of the NAO on North Atlantic surface temperature. Climate Dynamics, 19(1), 17–30. http://doi.org/10.1007/s00382-001-0211-y

Stahl, K., Hisdal, H., Hannaford, J., Tallaksen, L. M., Van Lanen, H. A. J., Sauquet, E., … Ĵodar, J. (2010). Streamflow trends in Europe: Evidence from a dataset of near-natural catchments. Hydrology and Earth System Sciences, 14(12), 2367–2382. http://doi.org/10.5194/hess-14-2367-2010

Terray, L., & Cassou, C. (2002). Tropical Atlantic Sea Surface Temperature Forcing of Quasi-Decadal Climate Variability over the North Atlantic–European Region. Journal of Climate, 15, 3170–3187.

Torrence, C., & Compo, G. P. (1998). A practical guide to wavelet analysis. Bull. Am. Meteorol. Soc., 79, 61–78. http://doi.org/10.1175/1520-0477(1998)079<0061:APGTWA>2.0.CO;2

Trenberth, K. E., Smith, L., Qian, T., Dai, A., & Fasullo, J. (2007). Estimates of the Global Water Budget and Its Annual Cycle Using Observational and Model Data. Journal of Hydrometeorology, 8(4), 758–769. http://doi.org/10.1175/JHM600.1

Trigo, R. M., Pozo-Vazquez, D., Osborn, T. J., Castro-Diez, Y., Gamiz-Fortis, S., & Esteban-Parra, M. J. (2004). North Atlantic oscillation influence on precipitation, river flow and water resources in the Iberian Peninsula. International Journal of Climatology, 24(8), 925–944. http://doi.org/10.1002/joc.1048

Wilson, D., Hannah, D. M., & McGregor, G. R. (2013). A large-scale hydroclimatological perspective on western European river flow regimes. Hydrology Research, 44(5), 809–833. Retrieved from http://hr.iwaponline.com/content/44/5/809.

FIGURE CAPTIONS

Figure 1- The Seine river and its catchment in northern France.

Figure 2- Continuous wavelet transforms of precipitation (A), streamflow (B) time series. A color scale (here, blue to red from minimum to maximum power) is used to identify the regions of this time/scale space were the signal displays amplitude. Thick black contour lines delimit the regions that are statistically significant at the 95% confidence limit when tested against a red noise model [AR(1)] computed for each spectrum as described in Torrence and Compo (1998). The white dashed line corresponds to the cone of influence under which edge effects become important and cause variance to be underestimated. Regions displaying power on the spectra are located on the spectra for periods of annual, interannual and interdecadal scales.

Figure 3- Mutiresolution decomposition of the monthly precipitation time series, using the so-called, redundant, maximum-overlap discrete wavelet transform. Wavelet detail at scale *i* is labeled *Di*, and the last component at level *j* that is no longer to be decomposed (the so-called "approximation" or "smooth") is referred to as *Sj*.

Figure 4- Same as Fig.3 for streamflow.

Figure 5- Composite maps of SLP generated for each scale based on precipitation variability. Statistically significant regions (Student t-test with a 95% confidence limit) are indicated within dashed lines.

Figure 6- Same as Fig.5 for streamflow.

Figure 7- Spatial distribution of regression coefficients of the multiple linear regression model based on 8 EOFs of SLP as predictor and precipitation as predictand. Here, the multiple linear regression model actually involved each wavelet component of SLP field and precipitation time

series, in such a way that each map represents the SLP spatial predictor of precipitation at each time-scale. Only the first seven wavelet components are represented here.

Figure 8- multiresolution ESD (A) and ESD (B) models of monthly precipitation. Gray line: original observed data; black line: simulated time series.

Figure 9- Continuous wavelet transforms of simulated monthly precipitation time series achieved with ESD (A) and multiresolution ESD (B). The low-frequency variability above 2 years that characterized observed precipitation (Fig.3A) is well retrieved using multiresolution ESD.

Figure 10- ESD (gray) and multiresolution ESD (black) versus observed (connected points) precipitation (A) and streamflow (B) time series, aggregated annually. The multiresolution ESD simulation performs well in reproducing the interannual variability of the time series. In the case of streamflow, the ESD simulation alone completely fails in reconstructing interannual variations. (C): same as (A) but using the period 1950-1998 for calibration and 1999-2007 for validation; the multiresolution ESD model (black) was successful in predicting observed high precipitation amounts of the late 90's-early 2000 period (connected points). The ESD model (gray) was not able to catch the high amplitudes of observed precipiation during this same period.

Figure 11- Interannual ~1.5/1.9-yr, ~3.2-yr and interdecadal ~19.3-yr components of precipitation (A) and streamflow (B).

Figure 12 - Influence of the scale/wavelet function on the result of multiresolution ESD modeling. 10 least asymetric daubechies scale and associated wavelet functions with 2, 4, 6, 8, 10, 12, 14, 16 18 and 20 coefficients were used, showing no high dispersion of the 10 multiresolution ESD models generated.

TABLES

Table 1- Equivalent Fourier period, standard deviation and amplitude (expressed as percentage of total standard deviation of the original time series) of each component (i.e. wavelet details and smooth) of precipitation.

Table 2- Same as Table 2 for streamflow.


N
Celtic Sea
English Channel
English Channel
GERMANY
BELGIUM
LUXEMBOURG
CZECH REPUBLIC
SLOVAKIA
AUSTRIA
HUNGARY
SLOVENIA
FRANCE
SWITZERLAND
Bay of Biscay
CROATIA
BOSNIA AND HERZEGOVINA
Ligurian Sea
Gulf of Lion
ITALY
Adriatic Sea
MONTENEGRO
Gulf of Taranto
Tyrrhenian Sea
Legend
Seine River
Seine Watershed
0
500
1 000 km
Esri, HERE, DeLorme, MapmyIndia, © OpenStreetMap contributors, and the GIS user community

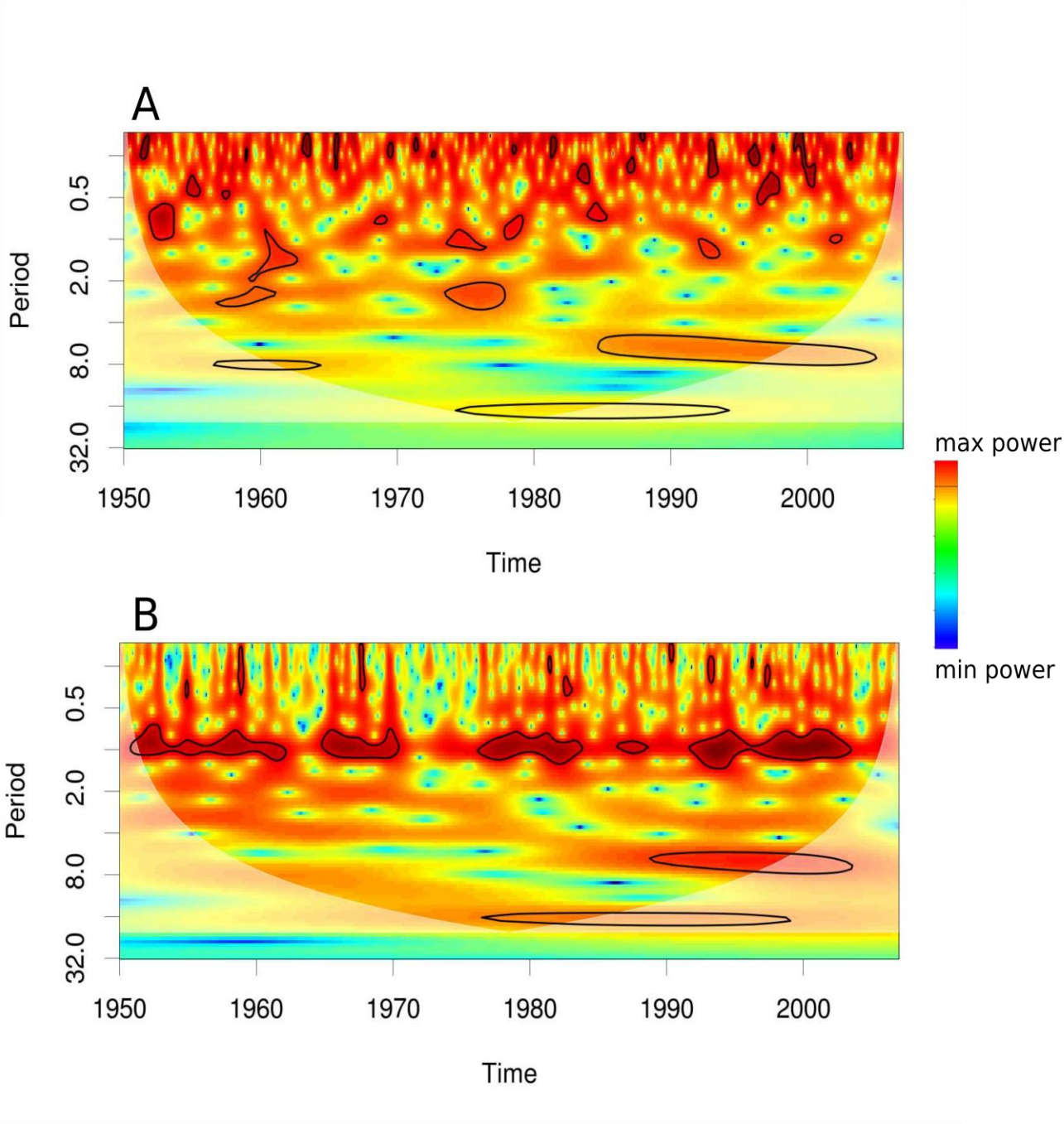
A
Period
0.5
2.0
8.0
32.0
1950
1960
1970
1980
1990
2000
Time
max power
min power
B
Period
0.5
2.0
8.0
32.0
1950
1960
1970
1980
1990
2000
Time

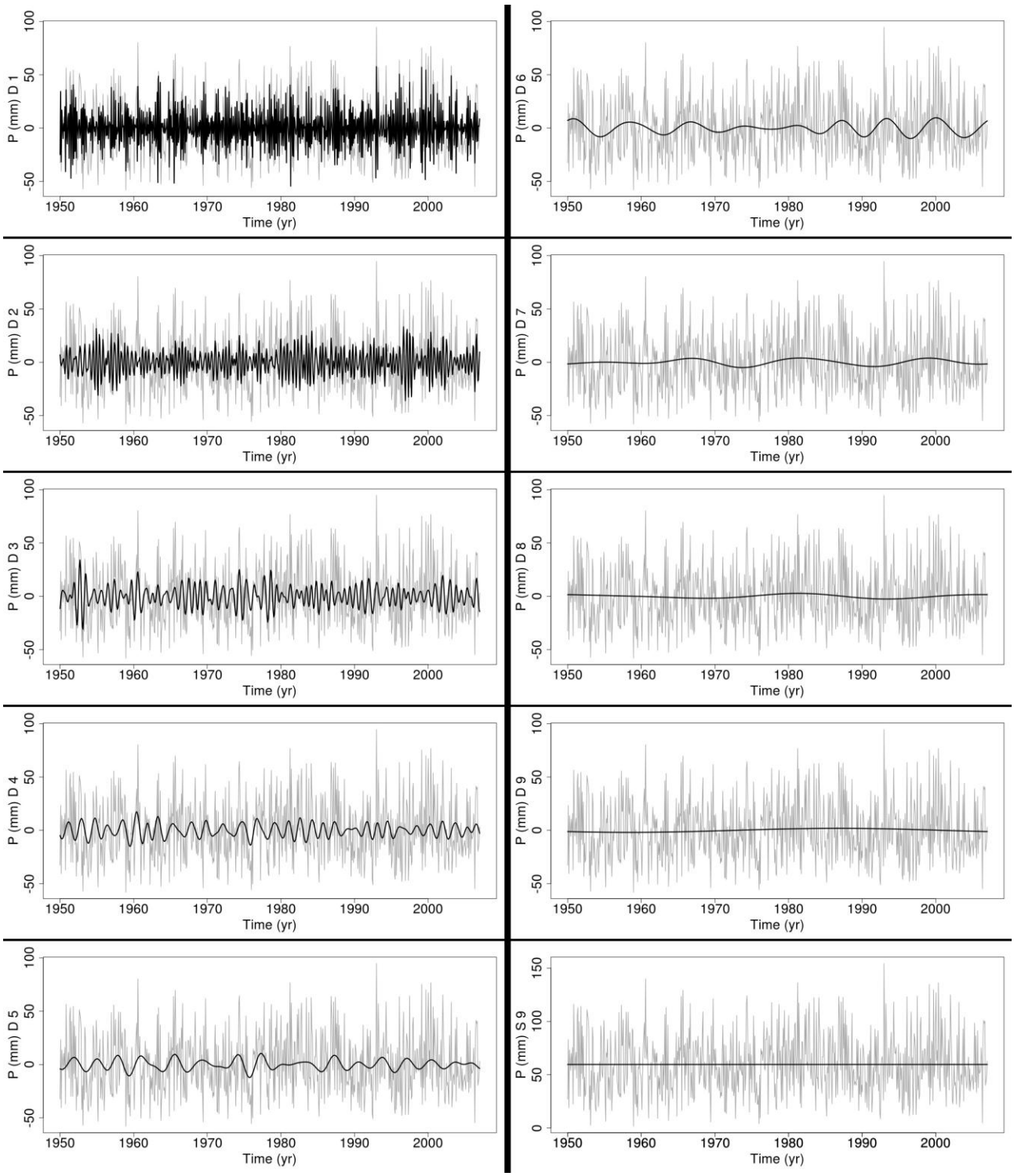
P (mm) D 1
P (mm) D 6
P (mm) D 2
P (mm) D 7
P (mm) D 3
P (mm) D 8
P (mm) D 4
P (mm) D 9
P (mm) D 5
P (mm) S 9
Time (yr)
1950
1960
1970
1980
1990
2000

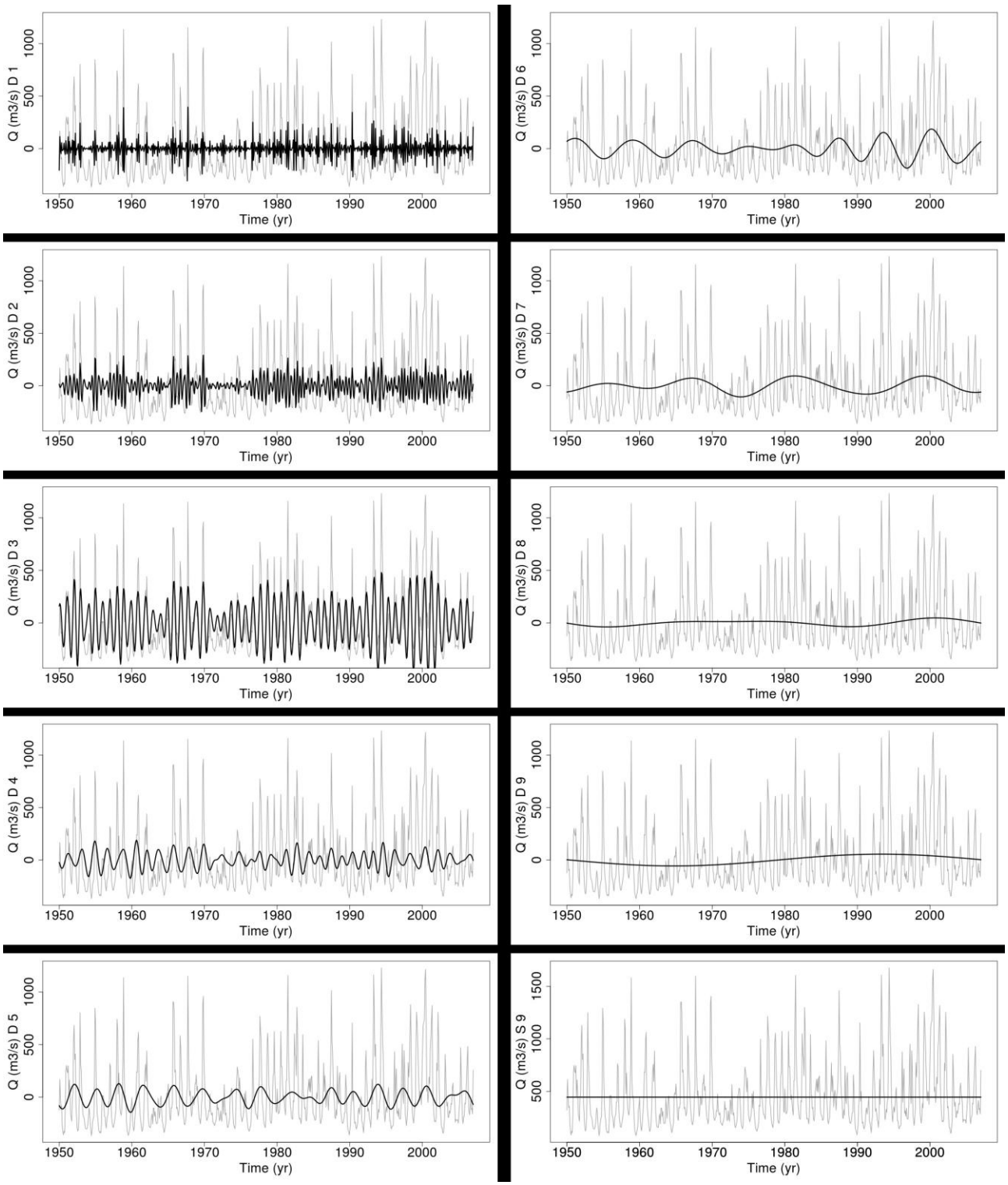
Q (m3/s) D 1
Q (m3/s) D 6
Q (m3/s) D 2
Q (m3/s) D 7
Q (m3/s) D 3
Q (m3/s) D 8
Q (m3/s) D 4
Q (m3/s) D 9
Q (m3/s) D 5
Q (m3/s) S 9
0
500
1000
1500
1950
1960
1970
1980
1990
2000
Time (yr)

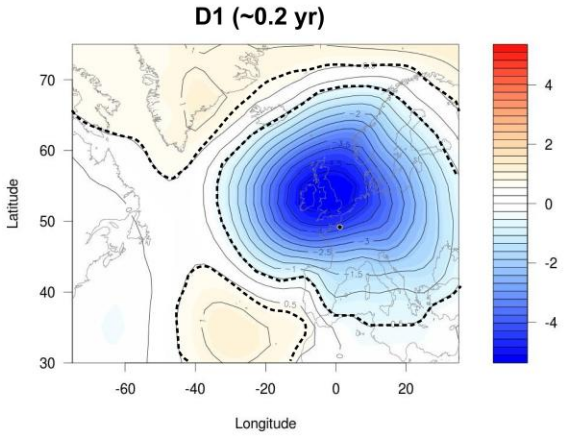
D1 (~0.2 yr)
Latitude
Longitude

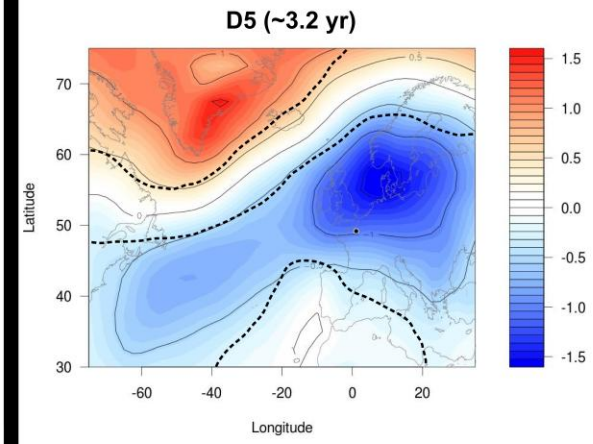
D5 (~3.2 yr)
Latitude
Longitude

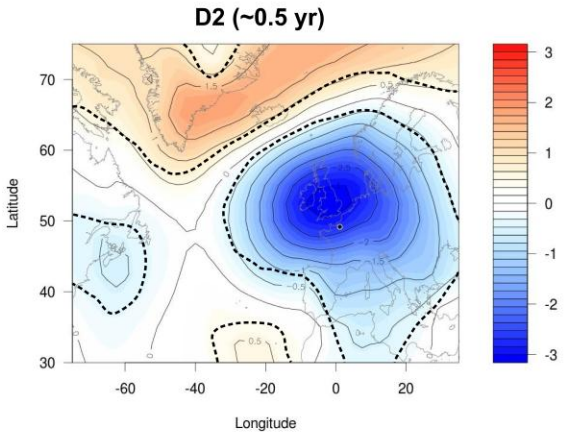
D2 (~0.5 yr)
Latitude
Longitude

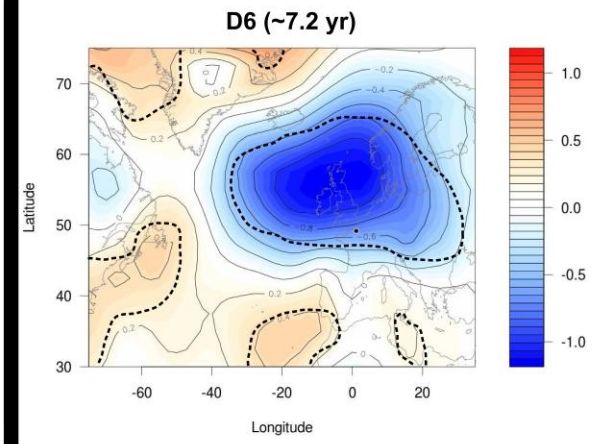
D6 (~7.2 yr)
Latitude
Longitude

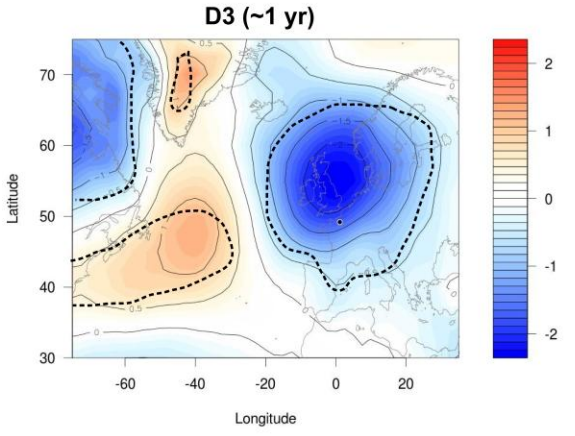
D3 (~1 yr)
Latitude
Longitude

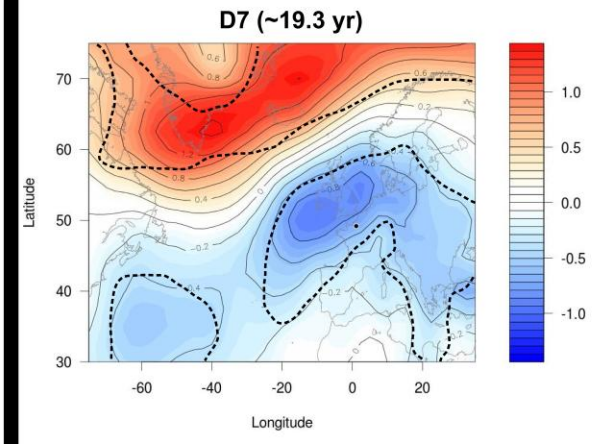
D7 (~19.3 yr)
Latitude
Longitude

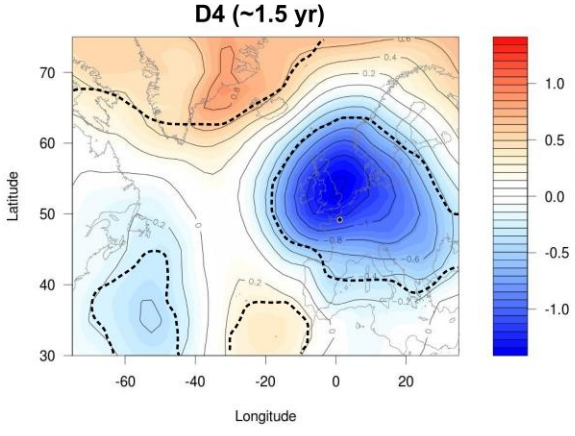
D4 (~1.5 yr)
Latitude
Longitude

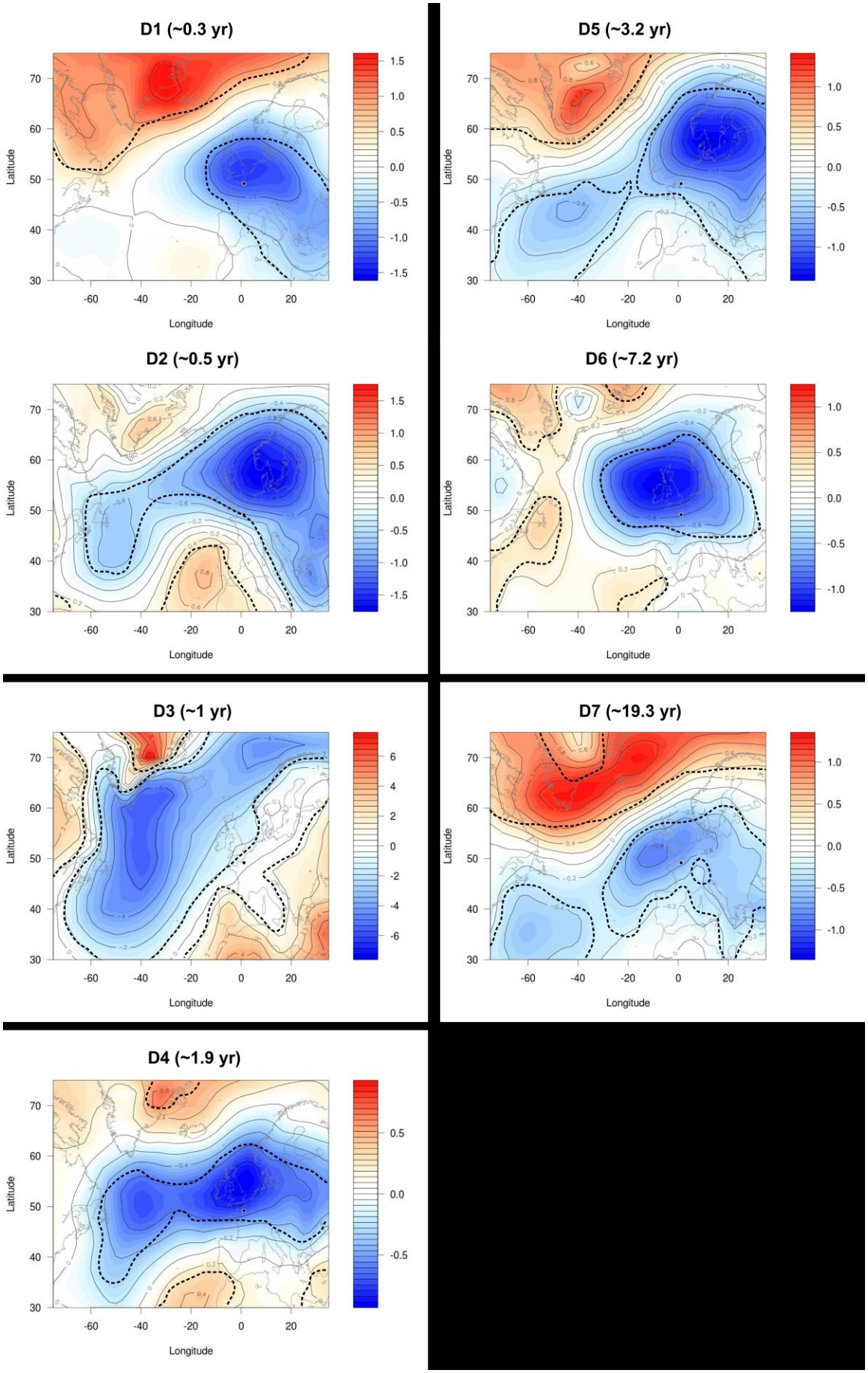
D1 (~0.3 yr)
D5 (~3.2 yr)
D2 (~0.5 yr)
D6 (~7.2 yr)
D3 (~1 yr)
D7 (~19.3 yr)
D4 (~1.9 yr)
Latitude
Longitude

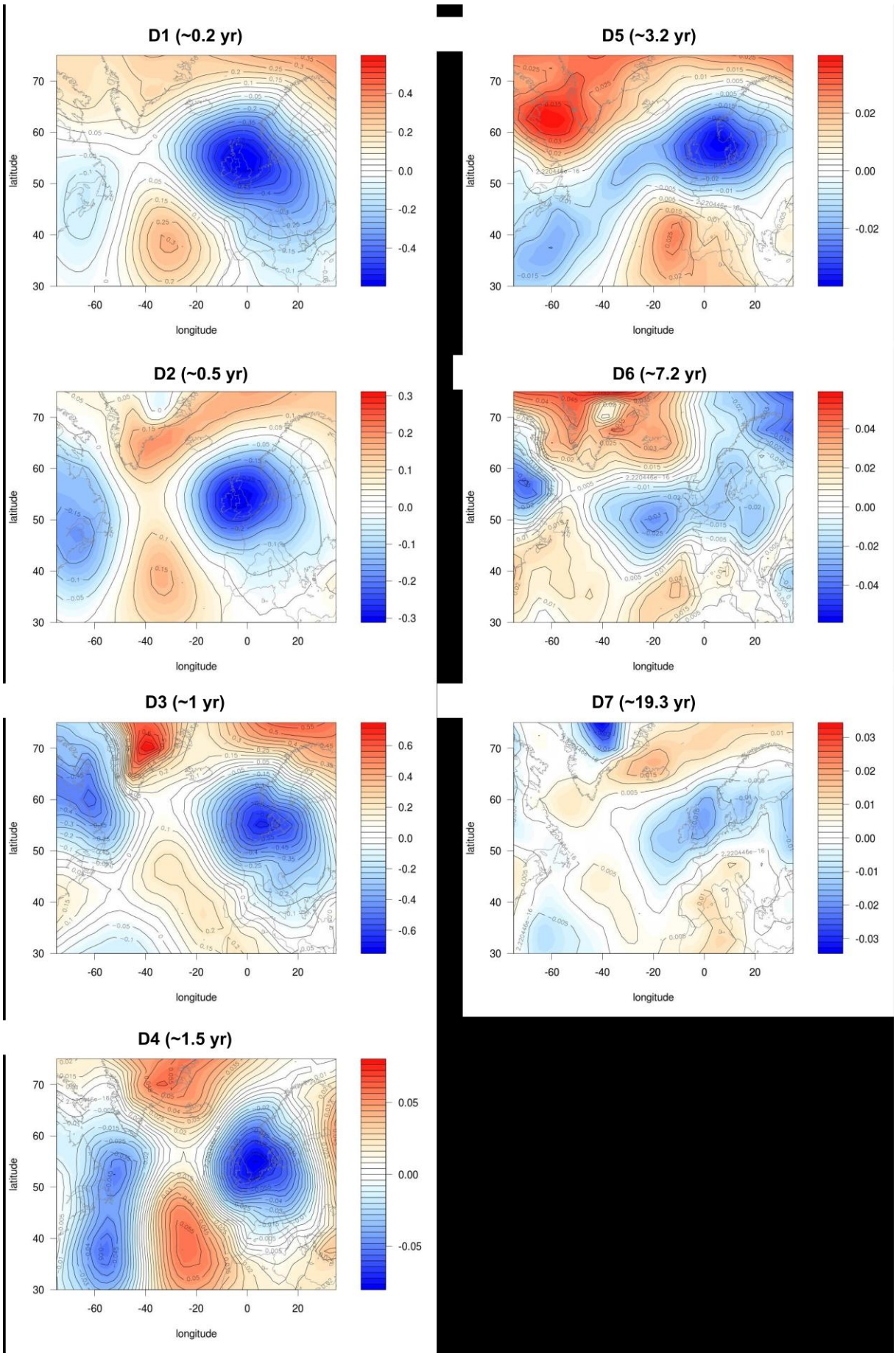
D1 (~0.2 yr)
D5 (~3.2 yr)
D2 (~0.5 yr)
D6 (~7.2 yr)
D3 (~1 yr)
D7 (~19.3 yr)
D4 (~1.5 yr)
latitude
longitude

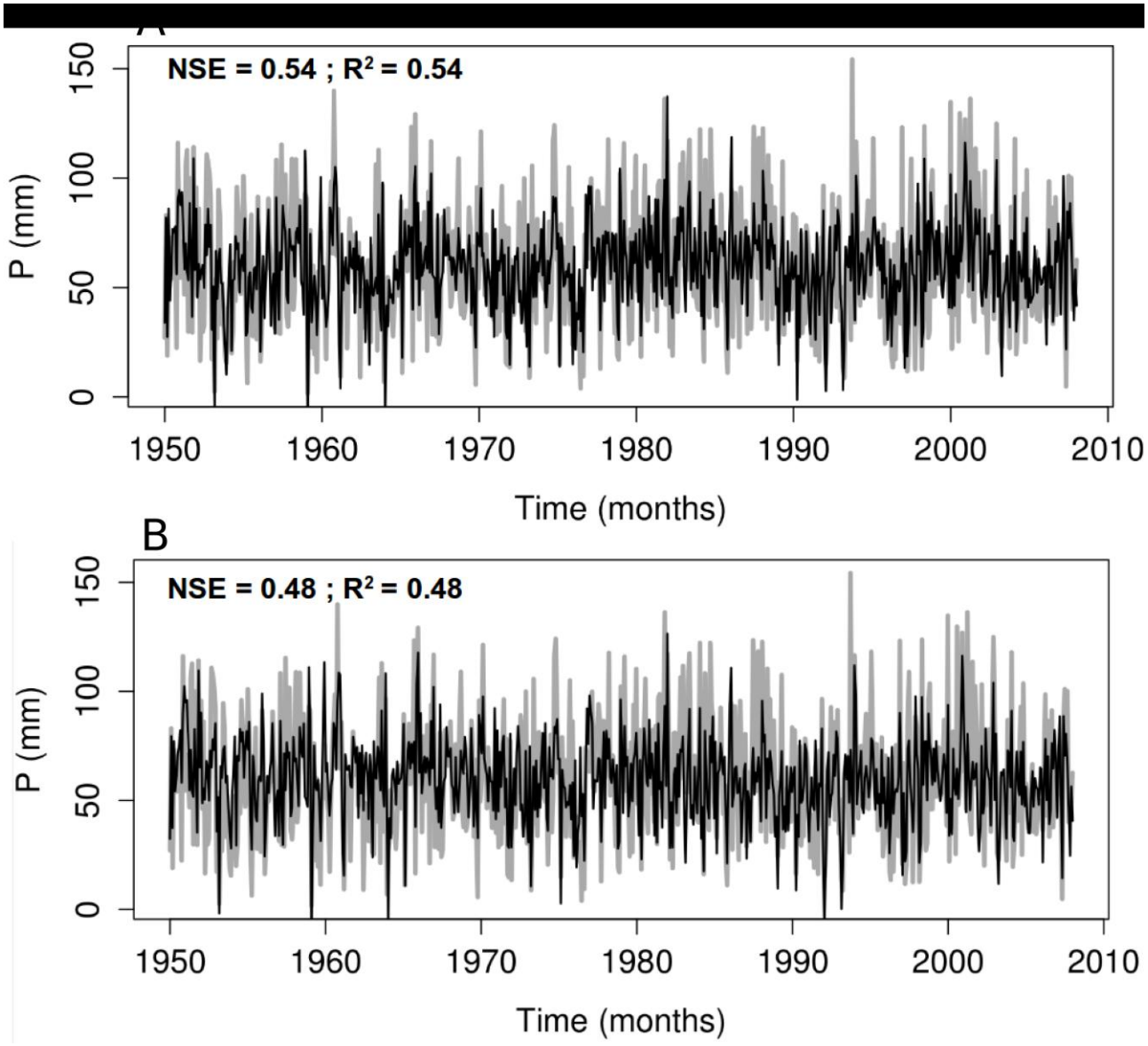
A
NSE = 0.54 ; R² = 0.54
P (mm)
0
50
100
150
1950
1960
1970
1980
1990
2000
2010
Time (months)
B
NSE = 0.48 ; R² = 0.48
P (mm)
0
50
100
150
1950
1960
1970
1980
1990
2000
2010
Time (months)

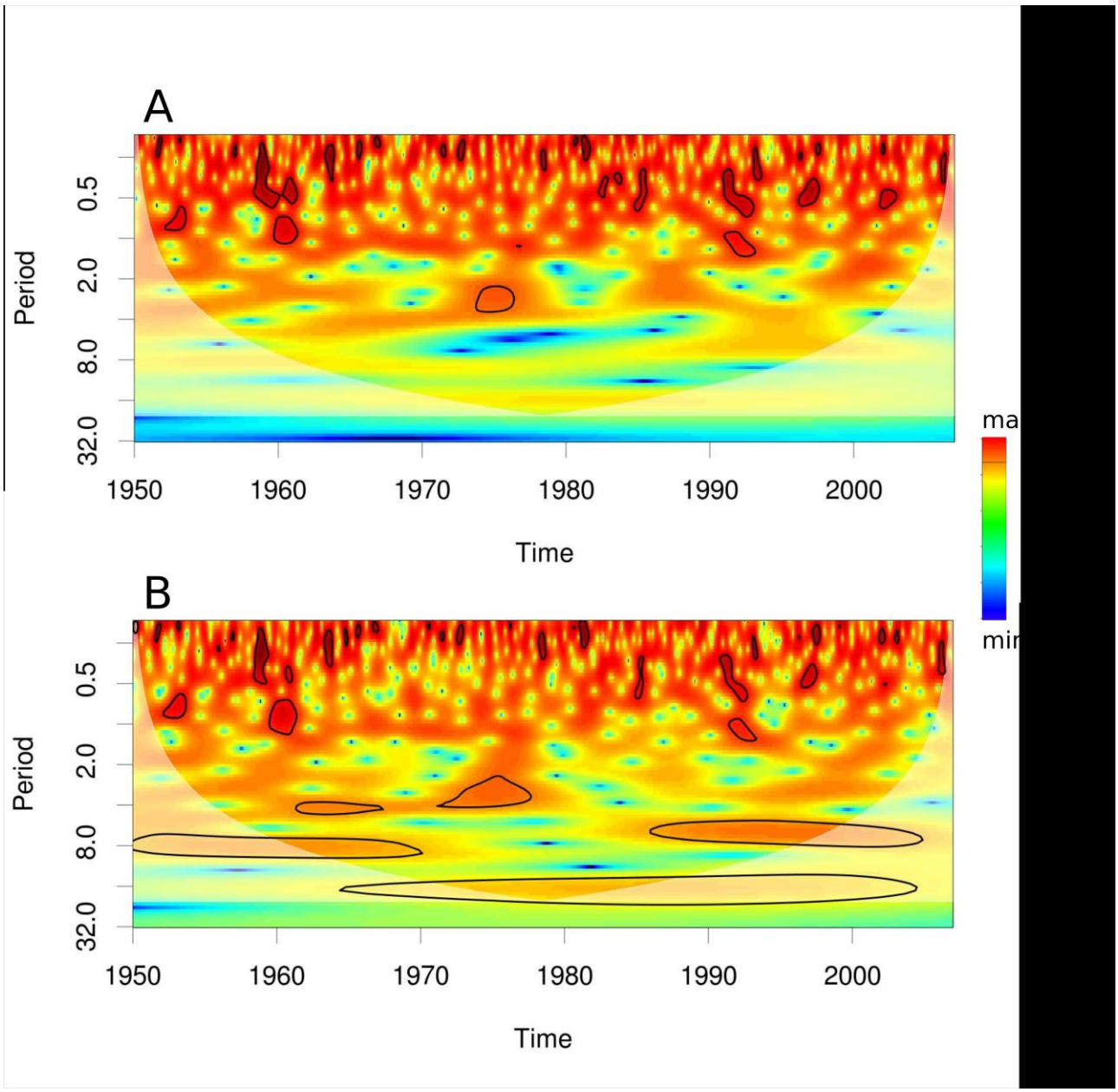
A
Period
0.5
2.0
8.0
32.0
1950
1960
1970
1980
1990
2000
Time
B
Period
0.5
2.0
8.0
32.0
1950
1960
1970
1980
1990
2000
Time

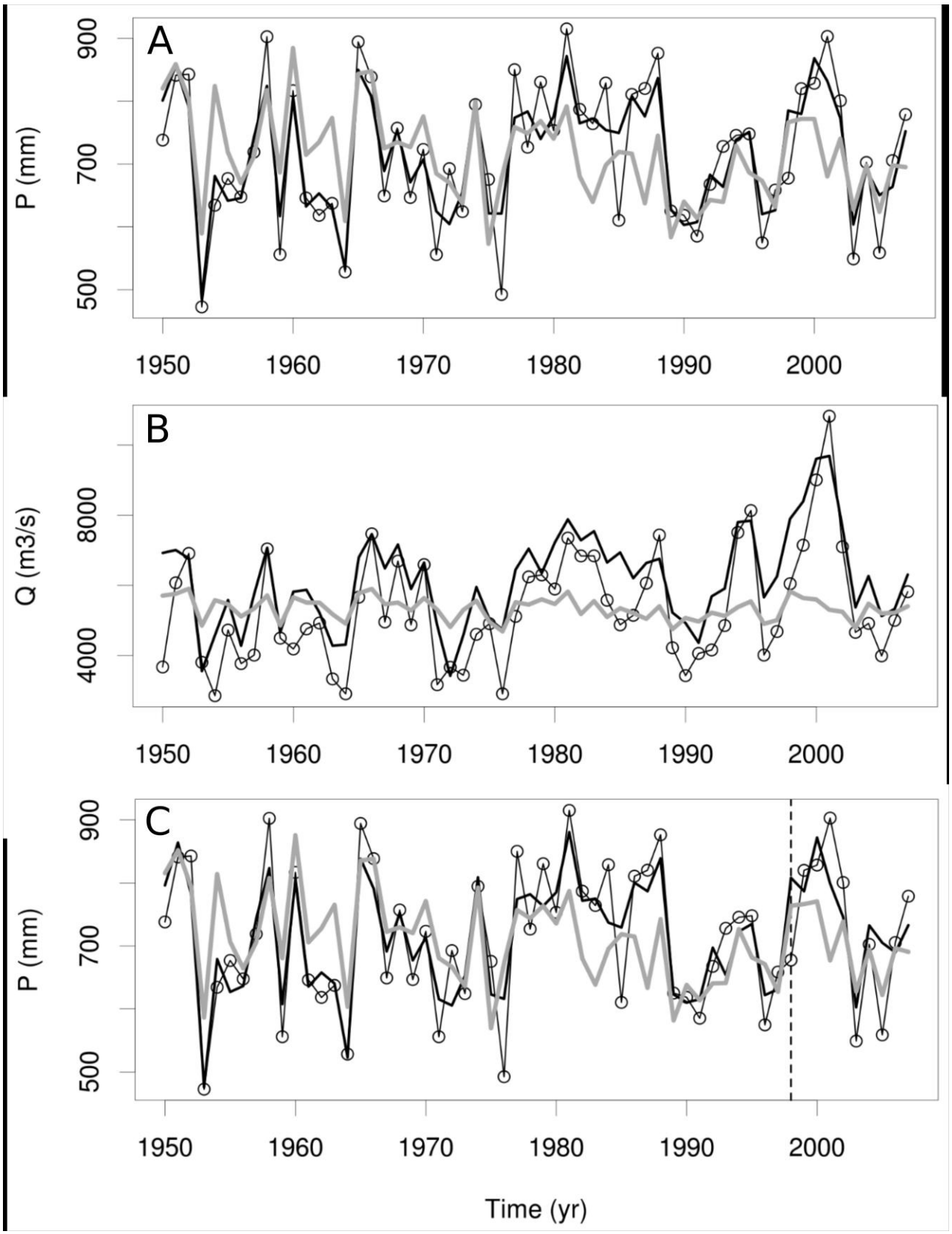
A
P (mm)
500
700
900
1950
1960
1970
1980
1990
2000
B
Q (m3/s)
4000
8000
1950
1960
1970
1980
1990
2000
C
P (mm)
500
700
900
1950
1960
1970
1980
1990
2000
Time (yr)

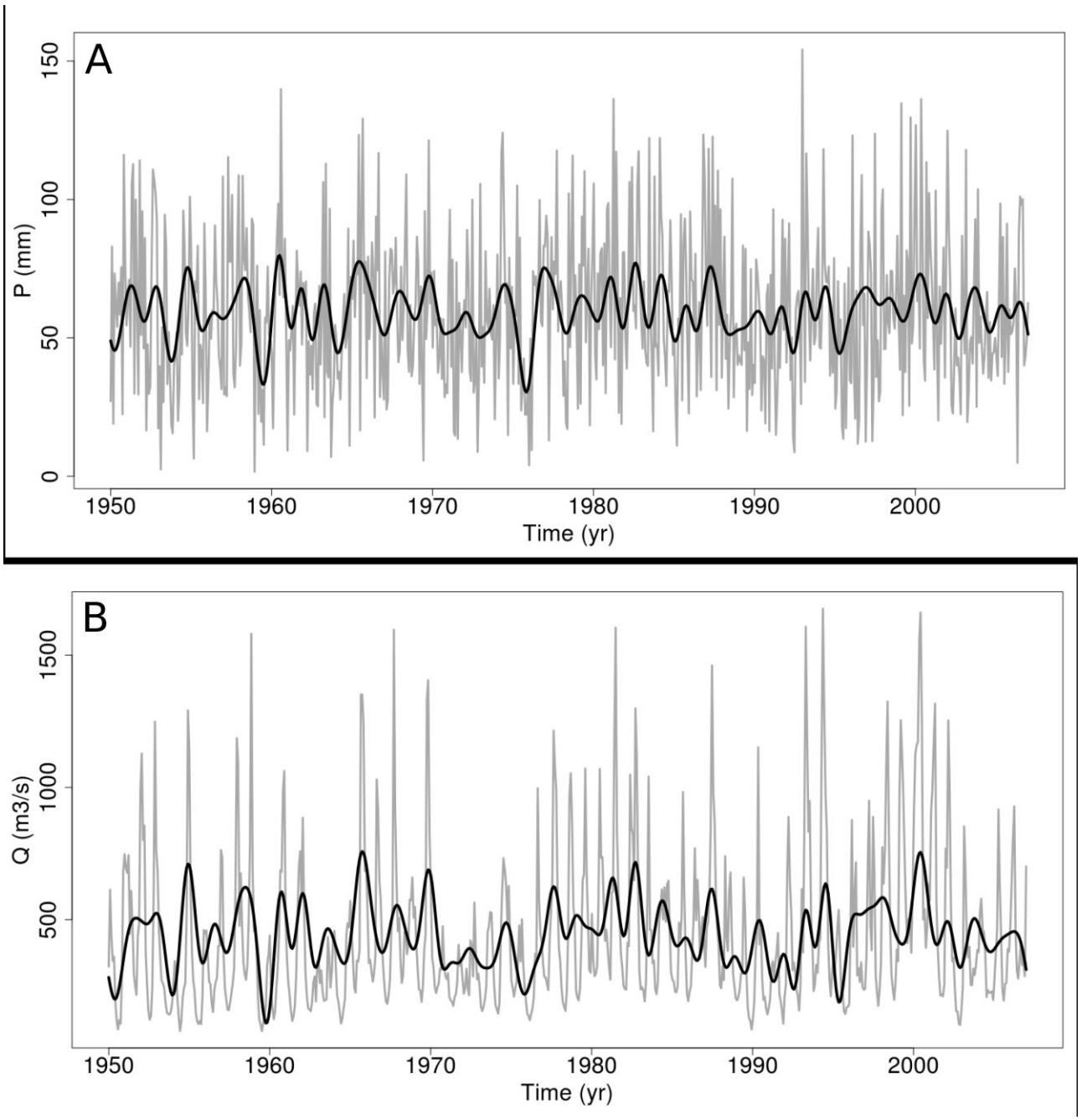
A
P (mm)
0
50
100
150
1950
1960
1970
1980
1990
2000
Time (yr)
B
Q (m3/s)
500
1000
1500
1950
1960
1970
1980
1990
2000
Time (yr)

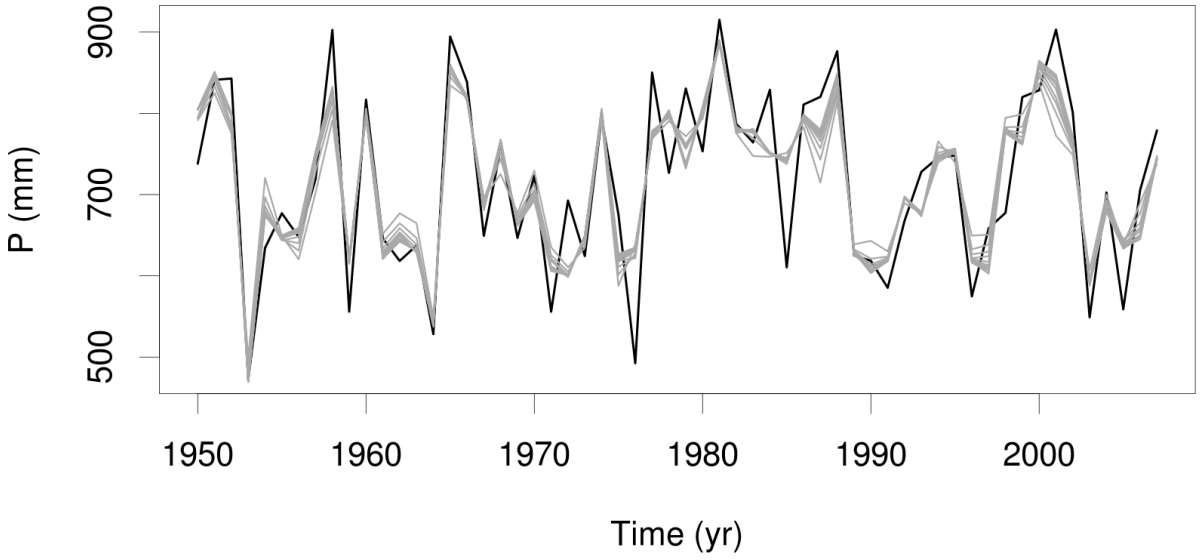
P (mm)
500
700
900
1950
1960
1970
1980
1990
2000
Time (yr)

Precipitation	D1	D2	D3	D4	D5	D6	D7	D8	D9	S9	Total
Fourier period (yr)	0.2	0.5	1.0	1.5	3.2	7.2	19.3	29.0	58.0	-	-
Standard deviation (mm)	18.3	10.6	8.2	5.4	4.1	4.4	2.2	1.5	1.2	0.0	28.0
Energy (%)	48.9	23.1	13.1	6.3	3.7	3.2	1.0	0.5	0.2	0.0	100

Streamflow	D1	D2	D3	D4	D5	D6	D7	D8	D9	S9	Total
Fourier period (yr)	0.3	0.5	1.0	1.9	3.2	7.2	19.3	29.0	58.0	-	-
Standard deviation (m^3/s)	79.1	83.4	181.2	67.8	58.3	67.3	49.1	25.0	35.4	0.6	299.0
Energy (%)	9.1	14.4	45.5	10.5	6.3	7.0	4.0	1.6	1.7	0.0	100

> Links between Sea Level Pressure and precipitation or streamflow were studied on Seine. > Links were investigated from high- to low-frequency components of the signals. > Links were found to be time-scale dependent. > Such findings might be useful for refining statistical downscaling models.